

Stiffness Modulation Exploiting Configuration Redundancy in Mobile Cable Robots

Xiaobo Zhou, Seung-kook Jun and Venkat Krovi

Abstract—In this paper, we investigate the modulation of task space stiffness of mobile cable robots with elastic cables. The elasticity is introduced via springs connected in series with non-extensible cables. The benefit of such series elastic cables include tension control without using force sensors and tension redistribution. However, elasticity also reduces positioning accuracy and makes the system more prone to disturbances. Therefore, careful stiffness modulation is needed for better performance. We exploit the configuration redundancy in mobile cable robots to optimize certain desired task space stiffness criterion. Both simulation and experimental results are presented for validation.

I. INTRODUCTION

Cable-driven parallel robots (cable robots), are formed by using variable length cables (instead of rigid links) connected to a payload platform. They have significantly improved workspaces as compared to traditional rigid link manipulators with high payload-to-weight ratio. Overall low cost and reliability contribute to their deployment in many real-world applications, such as heavy payload handling for manufacturing [1], extraterrestrial exploration [2], haptics [3], [4], large scale radio telescopes [5], [6], and load transport [7].

However, the high stiffness property of traditional rigid link parallel robots may be degraded due to the inevitable elasticity of cables, which is important for disturbance rejection in trajectory tracking tasks.

Stiffness [8] is a less studied but important characteristic directly related to the trajectory-following performance (and disturbance-rejection). Equally important are stiffness-control (or more generally impedance-control) strategies which seek to relate position error (and their time derivatives) to external-force exerted by the end-effector. Active impedance-control strategies have been developed to achieve desired open loop end-effector stiffness (impedance) using redundant actuation [9] for general robotic manipulators. This process becomes more challenging for constrained robotic systems with closed loops, and even more so for systems with unilateral constraints. However, possessing such control now offers an invaluable tool to dynamically-counteract certain classes of uncertain and unmodeled disturbances.

Despite the importance of stiffness, most of the previous work on cable robots assume a non-extensible (rigid/stiff)

cable model for simple analysis, with a notable exception of [10]. While it is true for many of the practical use cables available, i.e. the stiffness is high that the cable elongation may be ignored. However, as Merlet pointed out [11] it is impossible to use tension null space control for stiff cables, and hence he examined elasticity for cable model [12].

Current existing work on stiffness control of cable robots fall into two categories. The first way is to change tension, which is achieved by actuation redundancy from surplus cables. Internal cable tensions can be re-distributed among cables. Such actuation redundancy has been previously examined to achieve desired tension redistribution [13], [14]. While redundant actuation does not generate effective work in task space, it can be used to generate and change task space stiffness of the system. The Cartesian stiffness matrix can be written as $\mathbf{K}_X = \mathbf{K}_g + \mathbf{K}_c$, where $\mathbf{K}_g = \frac{\partial \mathbf{G}}{\partial \mathbf{x}} \mathbf{f}_p$, while the second component $\mathbf{K}_c = -\mathbf{G} \mathbf{K}_q \mathbf{G}^T$ (Note that \mathbf{K}_q is the joint space stiffness matrix). Chen and Kao [15] termed this mapping as Conservative Congruence Transformation (CCT). We see that Cartesian stiffness depends not only on changes in joint-stiffness, but also the system configuration and actuation-forces. Most importantly, for a given joint-stiffness and system-configuration, actively modulating the redundant actuation forces permits significant control over the achieved Cartesian stiffness. In Yu *et al.* [16], we presented active stiffness control schemes to take advantage of actuation redundancy, formulated as an optimization problem. However, such schemes are greatly limited when the number of extra actuation is less than the independent components of desired stiffness matrix. Hence, feasible solution may not always exist, which means desired stiffness can not be achieved in most designs under this *strict* criteria. As an alternative we have also explored guaranteeing minimal/lower bound on the stiffness by the control of the smallest eigenvalue [17] while operating under input constraints for simple cable robot systems. Such bounding of end-effector stiffness is intended to provide minimal guarantees of trajectory tracking and disturbance rejection performance. Both were validated via simulation.

The second option is to change the cable stiffness, which can be achieved by varying the stiffness of each individual cable. Nonlinear cable stiffness for passive impedance control has been previously explored [18]. Very recently, Yeo *et.al* [19] designed a variable stiffness add-on module for individual cables to enhance the overall stiffness of the cable robot.

We explore a third option – to change the configuration (i.e. via kinematic redundancy), which will be the direction

This work was supported in part by the National Science Foundation Grants IIS-1319084 and CNS-1314484

X. Zhou, S.-K. Jun and V. Krovi are with the Department of Mechanical and Aerospace Engineering, State University of New York at Buffalo, Buffalo, NY 14260 USA
 xzhou9, seungjun, vkrovi@buffalo.edu

that we pursue in this work. Most of existing cable robot work focus on conventional fixed-base cable robots, therefore do not have the freedom of reconfiguration. In our previous work [20], [21], [22], we added base mobility into the system which introduces configuration redundancy that may be used to redistribute tension, i.e. load sharing. In this paper, we continue along this path and show that the configuration redundancy can be used to modulate the stiffness matrix.

By connecting a spring into the non-extensible cable we introduce series elasticity into cable robots. Series elastic actuation [23] has been used in many other areas. By sacrificing some positioning accuracy, we gain better safety. For example, when hitting an obstacle, non-extensible cables may break and cause danger while the elasticity can absorb some of the impact energy. Also, impedance control for safe human robot interaction can be achieved. Additionally, the benefit of removing load cells from cable robots is possible. Tension can be regulated by regulating the extension of the spring.

Our proof of concept elastic mobile cable robot setup is shown in Fig. 1. There are two sliders L_{i1}, L_{i2} on each side i . The cable is fixed at slider L_{i1} on one side, routed through an idler pulley on slider L_{i2} , and then connected with a spring to the point mass end-effector, which is supported on a small platform with four caster wheels. The shining dots are reflective markers used by OptiTrack system for tracking. The linear slider is just a simple embodiment of a mobile base. Also the utilization of the linear sliders help to reduce cable length error introduced by the winches.

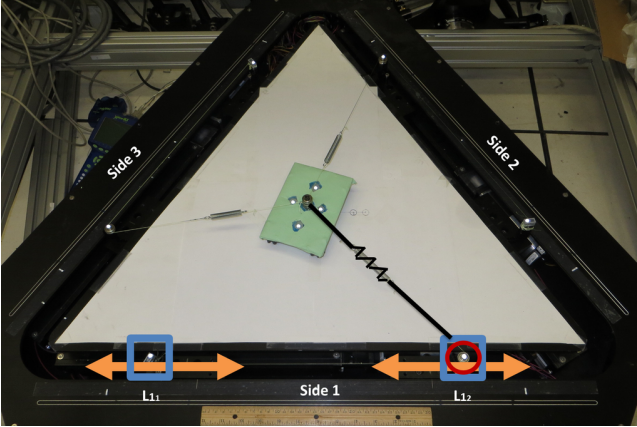


Fig. 1. Elastic mobile cable robot setup.

The paper is organized as follows: Section II presents the formulation of the system including Cartesian stiffness matrix; Section III discusses the configuration optimization for stiffness modulation and shows the benefit of the redundant base reconfiguration; We further generated feasible joint space motion for tracking payload trajectory with stiffness modulation along the way, and verified through experiment in Section IV; Finally, conclusion and future work is discussed in Section V.

II. FORMULATION

A schematic drawing of one side of the system is shown in Fig. 2. Synchronized moving of sliders L_{i1} and L_{i2} changes the cable base position (x_i, y_i) without changing the total cable length thus maintain the same cable tension. Moving L_{i1} relative to L_{i2} changes the spring extension and thereby changing the cable tension.

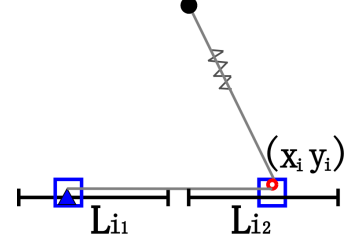


Fig. 2. Schematic drawing of one side of the robot.

A. Kinetostatics

With the cable elasticity, the kinematics problem becomes coupled with statics problems. For forward kinematics, given the slider positions, the end effector position will be dependent on the static equilibrium equation.

$$\mathbf{P}\mathbf{f} = -\mathbf{w}, \quad (1)$$

where \mathbf{w} is the external wrench exerted on the payload, \mathbf{P} is the pulling map derived following [21] to be

$$\mathbf{P} = \begin{bmatrix} -\cos \gamma_1 & -\cos \gamma_2 & -\cos \gamma_3 \\ \sin \gamma_1 & \sin \gamma_2 & \sin \gamma_3 \end{bmatrix} = \begin{bmatrix} \frac{x_1 - x_e}{\sqrt{(x_1 - x_e)^2 + (y_1 - y_e)^2}} & \frac{x_2 - x_e}{\sqrt{(x_2 - x_e)^2 + (y_2 - y_e)^2}} & \frac{x_3 - x_e}{\sqrt{(x_3 - x_e)^2 + (y_3 - y_e)^2}} \\ \frac{y_1 - y_e}{\sqrt{(x_1 - x_e)^2 + (y_1 - y_e)^2}} & \frac{y_2 - y_e}{\sqrt{(x_2 - x_e)^2 + (y_2 - y_e)^2}} & \frac{y_3 - y_e}{\sqrt{(x_3 - x_e)^2 + (y_3 - y_e)^2}} \end{bmatrix} \quad (2)$$

where (x_i, y_i) is the position of the slider pulley in world coordinate frame, γ_i is the angle of the cable in world frame at slider pulley location, (x_e, y_e) is the end-effector payload position. The tension in the cable is modeled as linear spring

$$f_i = k_i(\rho_i - l_{0i}) \quad (3)$$

where l_{0i} is the initial total length of the cable and spring, $k_i = \frac{k_{is}k_{ic}}{k_{is} + k_{ic}}$ is the stiffness of the cable, since the spring (with stiffness k_{is}) is connected in series with the cable and the cable itself is assumed in-extensible ($k_{ic} = +\infty$), therefore $k_i = k_{is}$; the total cable length including stretched spring

$$\rho_i = l_{i1} + l_{i2} + \sqrt{(x_i - x_e)^2 + (y_i - y_e)^2}. \quad (4)$$

where l_{i1} and l_{i2} are the traveling lengths of the sliders on i^{th} side.

The resulting end-effector position is computed numerically. Multiple solutions may be present due to nonlinearity, which need to be bounded. Methods such as interval analysis may be used for better solution [11].

For inverse kinematics, due to the kinematic redundancy, there are infinite slider positions for a given end-effector position, with different system properties. This is further addressed in Section III.

B. Stiffness Matrix

Starting from the pulling map

$$\mathbf{P}\mathbf{f} = -\underline{w}, \quad (5)$$

Cartesian stiffness matrix can be derived following [17] to be

$$\mathbf{K}_x = -\frac{\partial \mathbf{P}}{\partial \mathbf{x}_e} \mathbf{f} + \mathbf{P} \mathbf{K}_s \mathbf{P}^T = -\left[\frac{\partial \mathbf{P}}{\partial x_e} \mathbf{f}, \frac{\partial \mathbf{P}}{\partial y_e} \mathbf{f} \right] + \mathbf{P} \mathbf{K}_s \mathbf{P}^T \quad (6)$$

Looking at the matrix \mathbf{K}_x , it is obvious that there are three ways to change the stiffness: (1) change tension \mathbf{f} (actuation redundancy), which was examined by Yu *et.al* [17], [16]; (2) change cable stiffness \mathbf{K}_s , which was exploited by Yeo *et.al* [19]; and (3) change the pulling map \mathbf{P} (kinematic redundancy), which is detailed next.

III. STIFFNESS MODULATION

With the kinematic redundancy of mobile cable robots, we can optimize the configuration based on chosen objectives. For example, in [22], [20], we explored optimal tension distribution for load sharing. In this paper, since the cables are elastic, it is of interest to try optimizing the task space stiffness for better disturbance rejection.

A. Configuration Optimization

Resolving the kinematic redundancy is done through optimization. The general problem is formulated as the following

$$\begin{aligned} \text{minimize: } & C(\mathbf{l}) \\ \text{subject to: } & \mathbf{P}\mathbf{f} = -\underline{w} \\ & l_{i1} \in [l_{i1_{\min}}, l_{i1_{\max}}] \\ & l_{i2} \in [l_{i2_{\min}}, l_{i2_{\max}}] \\ & \Delta \rho_i \in (0, \Delta \rho_{i_{\max}}) \quad (i \in 1, 2, 3), \end{aligned} \quad (7)$$

where $C(\mathbf{l})$ is some performance measure cost function related to the cartesian stiffness matrix for various targets. The common constraints are force closure, slider limits and maximum extension of the springs, other constraints such as velocity limits can be added when needed as in the next section.

B. Isotropic Stiffness

One of our objectives is to have isotropic stiffness in both directions for providing equal resistance to disturbance. The cost function becomes

$$C(\mathbf{l}) = \frac{\lambda_{\max}}{\lambda_{\min}}, \quad (8)$$

where $\lambda = \text{eig}(\mathbf{K}_x)$ are the eigenvalues of the stiffness matrix. We note the positive definiteness is ensured by the force closure equilibrium condition, therefore no need to additionally enforce it as long as the equality constraint is not violated. This is used for the following optimization on the effect of base reconfiguration.

C. Benefit of Base Reconfiguration

To illustrate the effect of base reconfiguration, we show the following example for a comparison. The initial configuration is shown in Fig. 3. The stiffness matrix is drawn to scale (same for all the figures) in red ellipse, the green arrow is its major axis corresponding to the eigenvector associated with the larger eigenvalue, the yellow arrow shows the smaller eigenvalue.

We first increase the internal nullspace tensions amongst the cables to try to increase the stiffness. This is the approach adopted in paper [16], [17]. The result is shown in Fig. 4. As seen, the position of the base (l_{i2} sliders shown in small red circle) remain fixed, while the l_{i1} sliders (shown in blue square) move to stretch the spring to increase internal tension. The resulting stiffness ellipsoid is more round than the initial configuration, but not round enough.

Then we utilize the full potential of our system by optimizing the base l_{i2} slider positions along with internal tension to change stiffness. The result is shown in Fig. 5. It can be seen the base l_{i2} sliders move to different location, coupled with springs it is able to shape the stiffness ellipsoid close to a circle (isotropic).

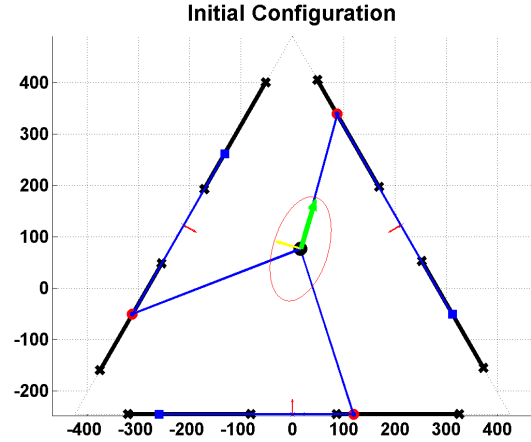


Fig. 3. Initial base configuration with stiffness ellipsoid drawn to scale.

Clearly, base reconfiguration allows the stiffness ellipsoid to be both larger and even. We see the effect of configuration change on the stiffness shaping is more significant than internal force regulation only.

D. Directional Stiffness

Additionally, we consider the problem of re-orienting the stiffness matrix, i.e. to align the major axis to a certain direction. This can be achieved by maximizing the angle between the two directions. Such problem may be formulated using the objective function as

$$C(\mathbf{l}) = |v^T u|, \quad (9)$$

where v is the eigenvector associated with the larger eigenvalue corresponding to the major axis of the ellipse, u is the desired unit direction vector.

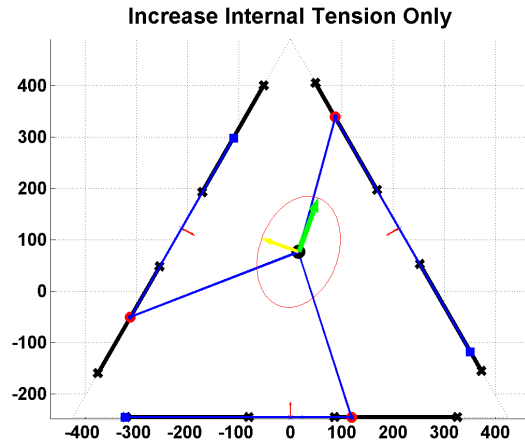


Fig. 4. Increase internal tension to shape stiffness.

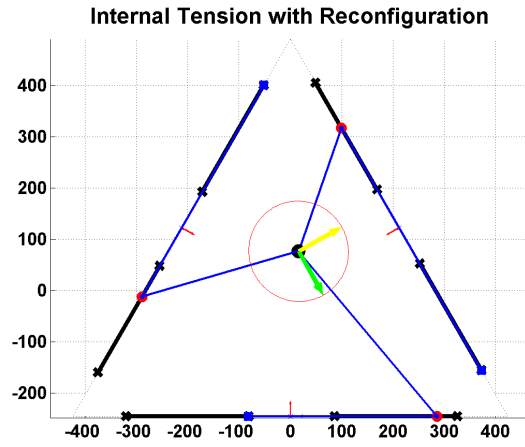


Fig. 5. Optimize both tension and position to shape stiffness.

An illustration example would be to track a line while reorienting the stiffness ellipsoid to be perpendicular to the trajectory to reject lateral disturbance. The result is shown in the following Fig. 6. From the left starting position, the major axis of the stiffness ellipsoid gets aligned with the direction of travel, as the robot moves and optimizes its configuration accordingly, the stiffness ellipse gets aligned perpendicular to the line of travel.

E. Maximum Stiffness

Another useful metric is proposed in [19], which ends up maximizing stiffness in both directions.

$$C(\mathbf{l}) = \frac{\lambda_1^2 \lambda_2^2}{\lambda_1^2 + \lambda_2^2}, \quad (10)$$

Strict isotropy is sacrificed for higher stiffness. This is desired when one wants the stiffness to be as high as possible. We use this metric to maximize stiffness along the trajectory in the next section, since we don't know the direction of unexpected disturbances.

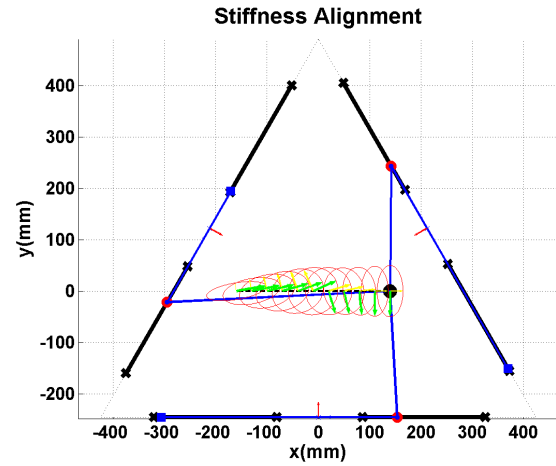


Fig. 6. Aligning the major axis (represented by a green arrow in the figure) of the stiffness ellipsoid to be perpendicular to the trajectory.

IV. TRAJECTORY TRACKING EXPERIMENTS WITH STIFFNESS MODULATION

The previous section showed how the kinematic redundancy can be used to optimize tension for one point in the workspace. Next we utilize it to modulate the stiffness during trajectory tracking.

We use the task of tracing a circle of radius 60mm centered at (0,0) counter clockwise starting from (-60,0) to illustrate the stiffness modulation effect.

The objective is to maximize stiffness, regardless of direction, thus the cost function in Eq. 10 is used for optimization. The resulting joint trajectory for maximizing stiffness is shown in Fig. 7

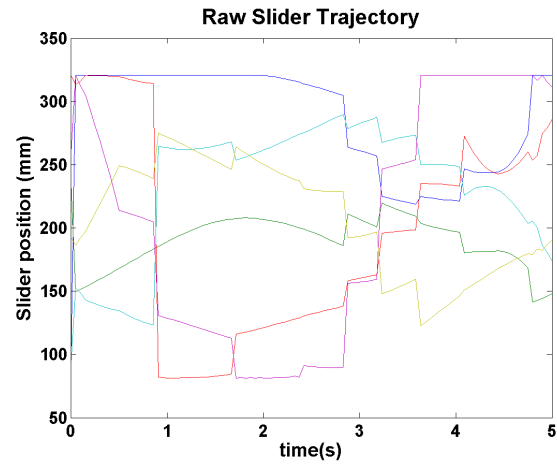


Fig. 7. Raw slider trajectory without velocity constraint.

Such joint trajectory is quite jerky, it is caused by two factors, one being the problem itself is nonlinear, therefore the optimization result will have multiple optimums; also the current solution is numerical which does not guarantee a specific optimum, therefore the solution may be jumping around; the second reason is there's no limit on the sliders,

it is assumed here the sliders can be repositioned instantaneously to optimal configuration, which is obviously not true for physical systems. We show next by adding practical constraints we can smooth the trajectory for deployment.

A. Trajectory Smoothing

The position trajectory passed to the lower level linear slider controls should be smooth, taking into account that physical limitations such as maximum velocity/acceleration are satisfied. Direct filtering of the trajectories should be avoided since the mapping from joint space to task space is highly nonlinear, doing simple filtering in joint space may result in unexpected task space movements. Instead, this should be done by incorporating the following additional constraints into the previous optimization problems.

$$\begin{aligned} \text{maximum velocity: } |\dot{l}_{i1}| &\leq V_{max} \\ |\dot{l}_{i1}| &\leq V_{max} \end{aligned} \quad (11)$$

Similarly acceleration even jerk constraints may be added if more smoothness is desired. We note here by introducing these physical limits, we are sacrificing the optimality, clearly due to speed limitations, it is not possible to get to optimum in one step, therefore the resulting are locally optimal, which are sufficient and acceptable in practical applications.

The resulting smooth trajectory is shown in Fig. 8, which is readily implementable. Further constraints such as acceleration level may also be added if desired.

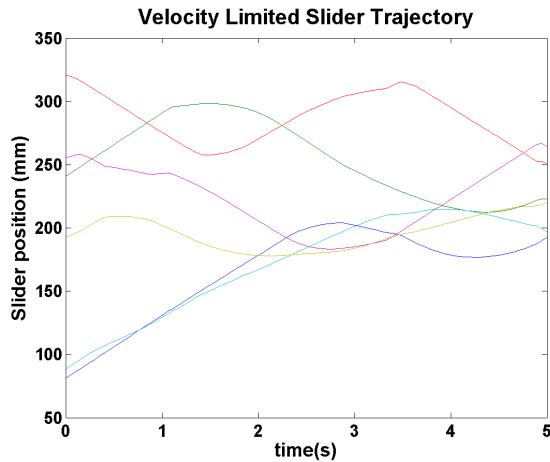


Fig. 8. Velocity constrained slider trajectory.

B. Experimental Setup

The experimental setup is shown in Fig. 9. OptiTrack cameras mounted on the frame are used to provide ground truth. The six linear sliders (two on each side) form an equilateral triangle. The distance from its geometric center to one side of the cable is 254mm, the range of travel of the sliders are limited to [40, 320]mm. The initial total cable lengths including springs at rest is [700, 700, 690]mm. The stiffness of the springs are obtained by linear fitting of the calibration data and are found to be [0.046, 0.055, 0.088]N/mm, relatively soft. The maximum extension of the spring is limited to 100mm for safety concerns.

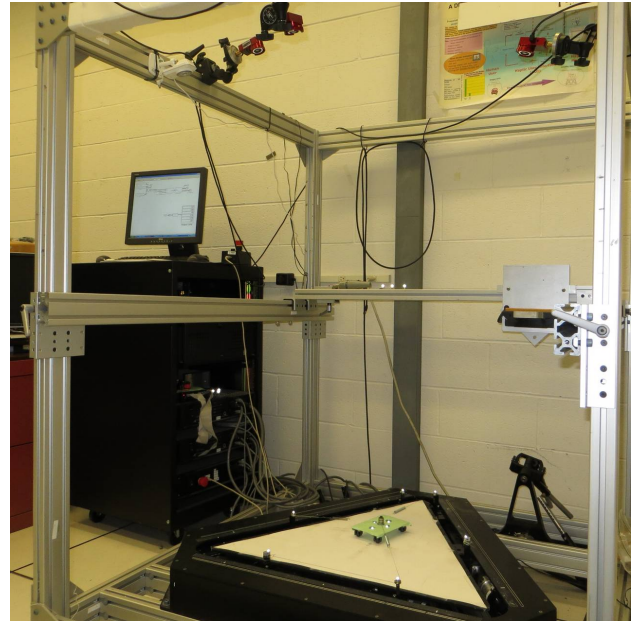


Fig. 9. Experimental setup.

C. Experimental Results

We show the experimental results of using redundancy to optimize stiffness. Two sets of experiments were performed. The first is without stiffness optimization, i.e. “soft” tracking. The second maximizes stiffness during tracing the circle using the result obtained in the previous subsection. For comparison, the result is shown in Fig. 10

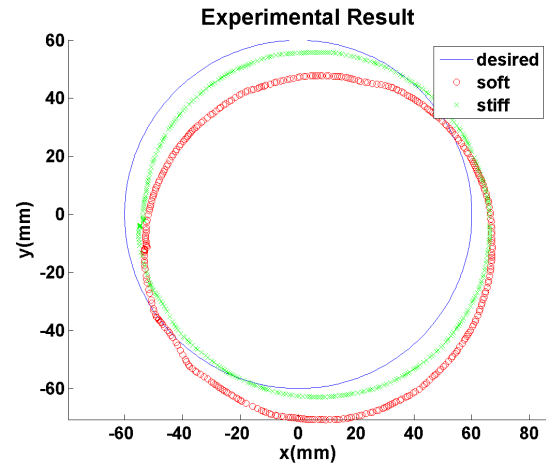


Fig. 10. Comparison of soft and stiff tracking.

The offset is caused by the uncertain geometric parameters as well as imperfect spring characteristics. However, if we look at the trajectory itself, it is clear that stiffer mode tracks better than soft mode. Also note this is just quasi-static joint space control, better control with task space feedback is underway. The accompanying video attachment shows more illustrative experimental results.

V. DISCUSSION

In this paper, we presented a elastic mobile cable robot and explored the modulation of its task space stiffness via both internal tension as well as utilizing the configuration redundancy. It is shown the kinematic redundancy allows for wider range of control over the Cartesian stiffness matrix than utilizing only internal tensions. We have shown that the stiffness can be actively modulated along a desired trajectory for better positioning accuracy.

The vibration induced by the springs, coupled with parametric uncertainties require better control for improved performance, which is the future direction we pursue.

REFERENCES

- [1] J. Albus, R. Bostelman, and N. Dagalakis, "The NIST ROBOCRANE," *Journal of Robotic Systems*, vol. 10, no. 5, pp. 709–724, 1993.
- [2] T. Huntsberger, A. Stroupe, H. Aghazarian, M. Garrett, P. Younse, and M. Powell, "TRESSA: Teamed robots for exploration and science on steep areas," *Journal of Field Robotics*, vol. 24, no. 11, pp. 1015–1031, November 2007.
- [3] S. Kawamura and K. Ito, "A new type of master robot for teleoperation using a radial wire drive system," in *Proceedings of the IEEE/RSJ International Conference on Intelligent Robots and Systems*, Yokohama, Japan, July 1993.
- [4] R. L. Williams II, "Cable-suspended haptic interface," *International Journal of Virtual Reality*, vol. 3, no. 3, pp. 13–21, 1998.
- [5] R. Nan, "Five hundred meter aperture spherical radio telescope (fast)," *Science in China Series G: Physics Mechanics and Astronomy*, vol. 49, no. 2, pp. 129–148, 2006.
- [6] G. Meunier, B. Boulet, and M. Nahon, "Control of an overactuated cable-driven parallel mechanism for a radio telescope application," *IEEE Transactions on Control Systems Technology*, vol. 17, no. 5, pp. 1043–1054, September 2009.
- [7] S.-R. Oh, J.-C. Ryu, and S. K. Agrawal, "Dynamics and control of a helicopter carrying a payload using a cable-suspended robot," *ASME Journal of Mechanical Design*, vol. 128, no. 5, pp. 1113–1121, September 2006.
- [8] R. Verhoeven, M. Hiller, and S. Tadokoro, "Workspace, stiffness, singularities and classification of tendon-driven stewart platforms," in *6th International Symposium on Advances in Robot Kinematics*, Salzburg, Austria, 1998, pp. 105–114.
- [9] B. J. Yi, R. A. Freeman, and D. Tesar, "Open-loop stiffness control of overconstrained mechanisms/robotic linkage systems," in *IEEE International Conference on Robotics and Automation*, vol. 3, Scottsdale, AZ, USA, 1989, pp. 1340–1345.
- [10] D. Surdilovic, J. Radojicic, and J. Kruger, *Geometric Stiffness Analysis of Wire Robots: A Mechanical Approach*, ser. Mechanisms and Machine Science. Springer Berlin Heidelberg, 2013, vol. 12, ch. 24, pp. 389–404.
- [11] J. Merlet, "The kinematics of the redundant n-1 wire driven parallel robot," in *Robotics and Automation (ICRA), 2012 IEEE International Conference on*, 2012, pp. 2313–2318.
- [12] J.-P. Merlet, "Analysis of wire elasticity for wire-driven parallel robots," in *Proceedings of EUROMES 08*, M. Ceccarelli, Ed. Springer Netherlands, 2009, pp. 471–478. [Online]. Available: http://dx.doi.org/10.1007/978-1-4020-8915-2_57
- [13] S.-R. Oh and S. K. Agrawal, "Cable suspended planar robots with redundant cables: controllers with positive tensions," *Robotics, IEEE Transactions on*, vol. 21, no. 3, pp. 457–465, 2005.
- [14] W. B. Lim, G. Yang, S. H. Yeo, S. K. Mustafa, and I. M. Chen, "A generic tension-closure analysis method for fully-constrained cable-driven parallel manipulators," in *Robotics and Automation (ICRA), 2009 IEEE International Conference on*, 2009, pp. 2187–2192.
- [15] S.-F. Chen and I. Kao, "Conservative congruence transformation for joint and cartesian stiffness matrices of robotic hands and fingers," *The International Journal of Robotics Research*, vol. 19, no. 9, pp. 835–847, 2000. [Online]. Available: <http://ijr.sagepub.com/content/19/9/835.abstract>
- [16] K. Yu, L.-F. Lee, and V. Krovı, "Simultaneous trajectory tracking and stiffness control of cable actuated parallel manipulator," in *Proceedings of the ASME Design Engineering Technical Conferences and Computer and Information in Engineering Conferences*, San Diego, California, USA, August–September 2009.
- [17] K. Yu, L.-F. Lee, C. P. Tang, and V. Krovı, "Enhanced trajectory tracking control with active lower bounded stiffness control for cable robot," in *Proceedings of the IEEE International Conference on Robotics and Automation*, Anchorage, Alaska, May 2010.
- [18] S. A. Migliore, E. A. Brown, and S. P. DeWeerth, "Novel nonlinear elastic actuators for passively controlling robotic joint compliance," *Journal of Mechanical Design*, vol. 129, no. 4, pp. 406–412, 2006, 10.1115/1.2429699.
- [19] S. Yeo, G. Yang, and W. Lim, "Design and analysis of cable-driven manipulators with variable stiffness," *Mechanism and Machine Theory*, vol. 69, no. 0, pp. 230 – 244, 2013. [Online]. Available: <http://www.sciencedirect.com/science/article/pii/S0094114X13001249>
- [20] X. Zhou, C. P. Tang, and V. Krovı, "Analysis framework for cooperating mobile cable robots," in *Robotics and Automation (ICRA), 2012 IEEE International Conference on*, may 2012, pp. 3128 –3133.
- [21] X. Zhou, C. Tang, and V. Krovı, *Cooperating Mobile Cable Robots: Screw Theoretic Analysis*, ser. Lecture Notes in Electrical Engineering. Springer Berlin Heidelberg, 2013, vol. 57, ch. 7, pp. 109–123.
- [22] X. Zhou, S. Jun, and V. Krovı, "Wrench reconfigurability via attachment point design in mobile cable robots," in *ASME 2013 International Design Engineering Technical Conferences and Computers in Engineering Conference (IDETC 2013)*, Portland, OR, 2013.
- [23] G. Pratt and M. Williamson, "Series elastic actuators," in *Intelligent Robots and Systems 95. 'Human Robot Interaction and Cooperative Robots', Proceedings. 1995 IEEE/RSJ International Conference on*, vol. 1, 1995, pp. 399–406 vol.1.